Spin state of iron in Fe_3O_4 magnetite and h-Fe_3O_4

Amelia Bengtson,[1,2] Dane Morgan,[1,*] and Udo Becker[2]

[1]*Department of Materials Science and Engineering, University of Wisconsin-Madison, Madison, Wisconsin 53706, USA*

[2]*Department of Earth and Environmental Sciences, University of Michigan, Ann Arbor, Michigan 48109, USA*

(Received 7 March 2012; revised manuscript received 12 October 2012; published 22 April 2013)

The high-pressure behavior of magnetite has been widely debated in the literature. Experimental measurements have found conflicting high-pressure transitions: a charge reordering in magnetite from inverse-spinel to normal-spinel [Pasternak *et al.*, J. Phys. Chem. Solids **65**, 1531 (2004); Rozenberg *et al.*, Phys. Rev. B **75**, 020102 (2007)], iron high-spin to intermediate-spin transition in magnetite [Ding *et al.*, Phys. Rev. Lett. **100**, 045508 (2008)], electron delocalization in magnetite [Baudelet *et al.*, Phys. Rev. B **82**, 140412 (2010); Glazyrin *et al.*, Am. Mineral. **97**, 128 (2012)], and a structural phase transition from magnetite to h-Fe_3O_4 [Dubrovinsky *et al.*, J. Phys.: Condens. Matter **15**, 7697 (2003); Fei *et al.*, Am. Mineral. **84**, 203 (1999); Haavik *et al.*, Am. Mineral. **85**, 514 (2000)]. We present *ab initio* calculations of iron's spin state in magnetite and h-Fe_3O_4, which help resolve the high-pressure debate. The results of the calculations find that iron remains high spin in both magnetite and h-Fe_3O_4; intermediate-spin iron is not stable. In addition, magnetite remains inverse-spinel but undergoes a phase transition to h-Fe_3O_4 near 10 GPa. Magnetite has a complex magnetic ordering, multiple valence states (Fe^{2+} and Fe^{3+}), charge ordering, and different local Fe site environments, all of which were accounted for in the calculations. The lack of intermediate-spin iron in magnetite helps resolve the spin state of iron in perovskite, the major mineral in the lower mantle. In both magnetite and perovskite, x-ray emission spectroscopy (XES) measurements in the literature show a drop in satellite peak intensity by approximately half, which is interpreted as intermediate-spin iron. In both minerals, calculations give no indication of intermediate-spin iron and predict high-spin iron to be stable for defect-free crystals. The results question the interpretation of a nonzero drop in XES satellite peak intensities as intermediate-spin iron.

DOI: 10.1103/PhysRevB.87.155141 PACS number(s): 32.10.Dk, 75.30.Kz, 75.25.Dk

I. INTRODUCTION

Magnetite (Fe_3O_4) has been of interest throughout history because it is one of the most magnetic naturally occurring minerals and is important for paleomagnetic measurements and past continent reconstruction.[1] Magnetite can also be found at higher pressures in the mantle wedge of subduction zones[2] formed as a byproduct of serpentinization of olivine.[3] In addition, electrical resistivity measurements in magnetite are useful for interpreting magnetotelluric measurements of the mantle.[4]

The high-pressure structural, electronic, and magnetic properties of Fe_3O_4 are not well characterized, and the complex coupling of iron spins contributes to these properties. Changes in magnetic, spin, and structural states alter density, elasticity, and electrical conductivity[5] and thus have an influence on interpretation of magnetotelluric measurements. In addition, changes that occur in the electronic or magnetic structure of Fe_3O_4 at high pressure could reset magnetic ordering in meteorites that collide at high pressure, therefore complicating the interpretation of paleomagnetic data.[6]

Fe_3O_4 has recently been suggested to undergo a transition from high-spin (HS) to an intermediate-spin (IS) state on some of the Fe atoms.[7] The nature of the possible IS transition in magnetite is important both for understanding Fe_3O_4 and for a more general understanding of the spin state of Fe in the Earth's lower mantle. Despite numerous experimental measurements and theoretical calculations, the spin state of Fe in perovskite, the dominant mineral in the lower mantle, is still under debate. X-ray emission spectroscopy (XES) measurements find the satellite peak intensity of Fe in perovskite drops to a nonzero value with increasing pressure, which is interpreted as a transition from HS to IS Fe.[8] However, theoretical calculations do not support IS Fe in perovskite.[9–13] XES measurements in magnetite show a drop in satellite peak intensity similar to perovskite, suggesting the spin state of Fe in magnetite is also IS.[7] Calculations of the spin state of Fe in magnetite will therefore provide additional evidence to help settle the more general debate over whether IS Fe occurs in high-pressure Fe compounds.

At ambient pressure and temperature, magnetite has an inverse-spinel structure $[Fe^{3+}]_{TET}[Fe^{2+/3+}Fe^{2+/3+}]_{OCT}$ with a random distribution of Fe^{2+} and Fe^{3+} on the octahedral (OCT) site.[14] The charges average to an effective valence state of $Fe^{2.5+}$ on the OCT sites. In the literature, agreement exists that a transition occurs in Fe_3O_4 between 10–20 GPa, but there is lack of agreement as to the type of transition. ^{57}Fe Mössbauer spectroscopy measurements suggest the high-pressure phase goes through an inverse- $[Fe^{3+}]_{TET}[Fe^{2+/3+}Fe^{2+/3+}]_{OCT}$ to normal- $[Fe^{2+}]_{TET}[Fe^{3+}Fe^{3+}]_{OCT}$ spinel transition with increasing pressure (8–15 GPa at room temperature).[15,16] However, K-edge x-ray magnetic circular dichroism and XES measurements are interpreted as an Fe^{2+} transition on the OCT site from HS to IS at 12–16 GPa.[7] An additional hypothesis, based on x-ray diffraction measurements, is that Fe_3O_4 has a phase transition from magnetite ($Fd\bar{3}m$ symmetry, $[Fe^{3+}]_{TET}[Fe^{2+/3+}Fe^{2+/3+}]_{OCT}$, inverse spinel) to a new high-pressure phase, h-Fe_3O_4 ($Pbcm$ symmetry, $[Fe^{2+}]_{TET}[Fe^{3+}Fe^{3+}]_{OCT}$, normal spinel) between 10 and 20 GPa (300 K).[17–19] The h-Fe_3O_4 crystal structure is a $CaMn_2O_4$-type structure[18] (Fig. 1). No studies have yet been done on the spin state of Fe in h-Fe_3O_4. More recent x-ray diffraction measurements and Mössbauer spectroscopy

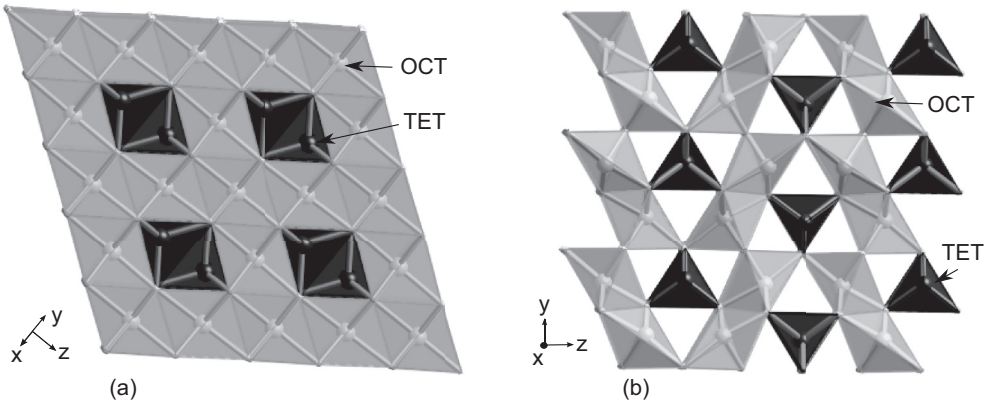

FIG. 1. (a) Magnetite. As an inverse spinel, the OCT site (light gray) is a statistical distribution of Fe^{2+} and Fe^{3+}, and the TET site (black) is Fe^{3+}. As a normal spinel, the OCT site is Fe^{3+}, and the TET site is Fe^{2+}. (b) h-Fe_3O_4, the high-pressure magnetite phase. The OCT site (light gray) is Fe^{3+} and the TET site (black) is Fe^{2+}.

experiments[4] as well as x-ray absorption spectroscopy and Fe K-edge x-ray magnetic circular dichroism measurements[20] find magnetite remains inverse spinel up to 25 GPa. Above 15 GPa, the measurements suggest the Fe electrons delocalize,[4] exhibiting a continuous decrease in moment[20] rather than undergoing a spin transition.

The measurements just discussed suggest four possible and quite different transitions with pressure: charge reordering in magnetite (inverse-spinel to normal-spinel), spin transition in magnetite (HS to IS), electron delocalization in magnetite, or a structural transition to a new phase (magnetite to h-Fe_3O_4). The goal of this paper is to calculate, using quantum-mechanical *ab initio* methods, the spin state of Fe as a function of pressure in Fe_3O_4 magnetite and h-Fe_3O_4. Because spin is linked to valence and site occupancy (and possibly magnetic ordering), multiple combinations of spin and ordering in both magnetite and h-Fe_3O_4 need to be explored. This work will both help elucidate the proposed pressure transitions that are actually occurring and the possibility of IS Fe in magnetite. Section II describes the computational methods, including the *ab initio* details and the different magnetic and spin states considered. Section III gives the results for magnetic and spin-state behavior of each structure of interest, including inverse spinel (Sec. III A), normal spinel (Sec. III B), and h-Fe_3O_4 (Sec. III C). The implications of these results for the stable phase as a function of pressure are given in Sec. III D, and Sec. III E provides useful elastic constant data.

II. METHODS

This study used density functional theory (DFT) methods as implemented in the Vienna *Ab initio* Simulation Package (VASP).[21] VASP calculations were performed with the projector-augmented wave method (electronic configuration: $2s^2\,2p^4$ for oxygen, $3p^6\,3d^7\,4s^1$ for Fe)[22] using the generalized gradient approximation (GGA) exchange-correlation with the Perdew–Burke–Ernzerhof parameterization[23] and a cutoff energy for the plane-wave basis functions of 600 eV. A $2 \times 2 \times 2$ Monkhorst–Pack k-point mesh was used for sampling the Brillouin zone of the reciprocal space for all structures. All k-point meshes and energy cutoffs were chosen to have a convergence of less than 0.005 eV in energies and 0.02 $Å^3$/atom in volume. A Hubbard U parameter[10] was applied to provide more accurate electronic structure for the localized d-orbitals and was necessary to stabilize distinct Fe^{2+} and Fe^{3+} atoms.[24] The invariant spin-polarized GGA + U scheme was used,[25] and U was added to Fe atoms only. We used U, the onsite Coulomb interaction parameter, equal to 4.6 eV and J, the effective on-site exchange interaction parameter, equal to 0.544 eV, consistent with previous work on Fe_3O_4.[24]

All calculations were performed as spin polarized. Individual moments were allowed to relax, and the total net moment of the cell was fixed. The spin and magnetic arrangements were created by setting initial magnetic moments on each atom and fixing the total net moment of the cell. Spins on the individual atoms were allowed to fully relax in the calculations. In some cases, a desired spin state with a given fixed total moment relaxed to another spin state with the same total net moment. Details on fixed total net moments, initial moments, and final relaxed moments are given below.

A. Computational structural details

A central goal of this study was to calculate the spin state of Fe as a function of pressure in magnetite. The structure of magnetite may change with pressure, and therefore three structures were considered in the calculations in order to map the entire pressure space: inverse-spinel magnetite, normal-spinel magnetite, and h-Fe_3O_4 (Table I).

In the remainder of the paper, the following notation is used:

$$\left[(-)\,\mathrm{Fe}_{\mathrm{SPIN}}^{\mathrm{valence}}\,(-)\,\mathrm{Fe}_{\mathrm{SPIN}}^{\mathrm{valence}}\right]_{\mathrm{TET}} \times \left[(-)\,\mathrm{Fe}_{\mathrm{SPIN}}^{\mathrm{valence}}\,(-)\,\mathrm{Fe}_{\mathrm{SPIN}}^{\mathrm{valence}}\,(-)\,\mathrm{Fe}_{\mathrm{SPIN}}^{\mathrm{valence}}\,(-)\,\mathrm{Fe}_{\mathrm{SPIN}}^{\mathrm{valence}}\right]_{\mathrm{OCT}}.$$

where $[]_{\mathrm{TET/OCT}}$ denotes the spin, valence, and magnetic ordering for the TET/OCT sites (Fig. 1). A "$-$" in front of Fe denotes that the spin points in the opposite direction from Fe without a "$-$". Only collinear spins are considered. The superscript/subscript after the Fe marks the valence/spin of that Fe atom. Spin will be represented by HS, IS, and low spin (LS), and the magnetic moment for each spin and valence state is given in Table II. The six Fe atoms represent the six Fe atoms in the 14-atom primitive unit cell of Fe_3O_4.[17]

TABLE I. Three structures are explored in the calculations. Magnetite may undergo an inverse-spinel to normal-spinel transition with pressure. Magnetite may also undergo a phase transition to h-Fe_3O_4 with pressure. The spin state of Fe within all three structures is necessary to gain a complete understanding of the high-pressure spin states.

Low-pressure	High-pressure		
Magnetite, inverse spinel. $[Fe^{3+}]_{TET}[Fe^{2+}Fe^{3+}]_{OCT}$ *Imma* symmetry	Magnetite, normal spinel $[Fe^{2+}]_{TET}[Fe^{3+}Fe^{3+}]_{OCT}$ $Fd\bar{3}m$ symmetry	or	h-Fe_3O_4, normal spinel $[Fe^{2+}]_{TET}[Fe^{3+}Fe^{3+}]_{OCT}$ *Pbcm* symmetry High-pressure phase
Fig. 1(a)	Fig. 1(a)		Fig. 1(b)

1. *Magnetite at ambient conditions: inverse spinel*

Fe occupies both TET and OCT sites in magnetite (Fig. 1) at ambient conditions. The magnetism in magnetite is due to the ferrimagnetic ordering of Fe spins between the TET and OCT sites (Fig. 1). The known phases for magnetite at lower pressure include both a low-temperature monoclinic phase with ordered Fe^{2+} and Fe^{3+} and a disordered $Fd\bar{3}m$ symmetry structure. At 120 K (T_V) magnetite undergoes an electronic transition, the Verwey transition, which corresponds to a change in electrical conductivity[14] due to the transition:

$$[Fe^{3+}]_{TET}[Fe^{3+}Fe^{2+}]_{OCT} \xleftarrow{T<T_V} \xrightarrow{T>T_V} [Fe^{3+}]_{TET}[Fe^{2+/3+}Fe^{2+/3+}]_{OCT}.$$

When $T > T_V$, there is a statistical distribution of Fe^{2+} and Fe^{3+} with an average charge of $Fe^{2.5+}$ on the OCT sites leading to high electrical conductivity. For $T < T_V$, Fe^{2+} and Fe^{3+} become ordered on the OCT site, and, as a consequence, conductivity is lost.[14] Charge ordering has been confirmed by resonant x-ray diffraction experiments.[26,27] DFT calculations are technically at absolute zero, since the energy solution corresponds to the ground-state energy.

The focus of this study was on pressure-induced spin transitions in magnetite at room temperature for direct comparison with the experimental spin-transition study by Ding *et al.*[7] Ideally, both phases would be included for a complete study of the spin state with and without the effect of charge ordering. Instead, a single phase, the charge-ordered structure $[Fe^{3+}]_{TET}[Fe^{3+}Fe^{2+}]_{OCT}$, was used as an approximation of the true statistical distribution at room temperature. This was a necessary approximation to make the calculations practical and an acceptable approximation given the goal of the work to study the spin transition. Representing the random distribution of Fe^{2+} and Fe^{3+} atoms in the $T > T_V$ charge-disordered structure $[Fe^{3+}]_{TET}[Fe^{2+/3+}Fe^{2+/3+}]_{OCT}$ would require a large cell that is computationally impractical for this work. Furthermore, the pressure dependence of T_V is not yet clear, and at the higher pressures of the mantle, the charge-ordered structure may in fact be the most stable structure at temperatures of interest.

In terms of the accuracy of the approximation, both the monoclinic (charge-ordered) and $Fd\bar{3}m$ (charge-averaged) structures are clearly quite similar in energy, as the Verwey transition occurs at T_{Verwey} =120 K. This generally argues for charge ordering being a small contribution to the energy, on the order of just kT_{Verwey}~10 meV/Fe atom. The results of this study showed the energy scale of the HS to IS transition in magnetite is 1.01 eV/f.u. (~340 meV/Fe). Therefore, the energy change due to charge-ordering differences should not change the energetics of the spin transition enough to stabilize IS and, in general, would have negligible effects on the transitions of interest.

The charge-ordered inverse-spinel magnetite structure was created by starting with $Fd\bar{3}m$ symmetry and the experimental atomic positions [Fe(TET) 0.125 0.125 0.125, Fe(OCT) 0.5 0.5 0.5, O 0.2549 0.2549 0.2549, $a = b = c = 8.3965$, $\alpha = \beta = \gamma = 90^\circ$].[17,28] To allow for ordering of Fe^{2+} and Fe^{3+}, a 14-atom unit cell was created,[29] and the symmetry on the OCT site was reduced to *Imma* by making the fourth and fifth Fe atoms Fe^{2+}, consistent with Wenzel and Steinle-Neumann (2007). The choice of the *Imma* charge-ordered inverse-spinel magnetite structure was a practical approximation that allowed us to elucidate the magnetite spin behavior with minimal loss of accuracy.

TABLE II. Total number of unpaired electrons and magnetic moment (μ_B) for each spin state and valence state (Fe^{2+} and Fe^{3+}).

Valence	HS	IS	LS
Fe^{2+}	4	2	0
Fe^{3+}	5	3	1

2. *Magnetite at high pressure: normal spinel*

Magnetite may undergo an inverse-spinel to normal-spinel transition near 8 GPa,[15,16] which is near the possible spin-transition region; therefore, spin transitions should also be considered in normal spinel. The normal spinel structure was created from the experimentally identified atom positions for this structure in a 14-atom unit cell with $Fd\bar{3}m$ symmetry.[17] In the input file, all TET atoms were specified as Fe^{2+}, and all OCT atoms were specified as Fe^{3+} by setting their respective initial magnetic moments.

3. *Phase change in magnetite at high pressure: h-Fe_3O_4*

The high-pressure magnetite phase h-Fe_3O_4 has a $CaMn_2O_4$-type structure with the *Pbcm* space group,[18] with the magnetic ordering of Fe^{2+} on the TET site and Fe^{3+} on the OCT site $[Fe^{2+}]_{TET}[Fe^{3+}Fe^{3+}]_{OCT}$ [Fig. 1(b)]. Within the calculations, the *Pbcm* symmetry relaxes to $CaTi_2O_4$-type *Bbmm*,[29] consistent with Refs. 19 and 17. A 28-atom unit cell was used.

TABLE III. All possible magnetic arrangements in the 14-atom inverse-spinel magnetite cell. If the arrangement/spin is metastable, then the initial moments specified in calculation are *locally* metastable after the final relaxations. Otherwise, the initial moments are *not locally* metastable and relaxed to different individual moments with the same total net moment. Labels in () correspond to labels on Fig. 2(a).

	TET		OCT					
Magnetic ordering, all HS	Fe1	Fe2	Fe3	Fe4	Fe5	Fe6	Net moment	Locally metastable
Ferrimagnetic (mag1) $[-Fe^{3+}_{HS} - Fe^{3+}_{HS}]_{TET}[Fe^{3+}_{HS}Fe^{2+}_{HS}Fe^{2+}_{HS}Fe^{3+}_{HS}]_{OCT}$	−5	−5	5	4	4	5	8	Yes
Antiferromagnetic (NMM0) $[-Fe^{3+}_{HS}Fe^{3+}_{HS}]_{TET}[-Fe^{3+}_{HS}Fe^{2+}_{HS} - Fe^{2+}_{HS}Fe^{3+}_{HS}]_{OCT}$	−5	5	−5	4	−4	5	0	Yes
Ferrimagnetic (NMM2) $[Fe^{3+}_{HS} - Fe^{3+}_{HS}]_{TET}[Fe^{3+}_{HS} - Fe^{2+}_{HS} - Fe^{2+}_{HS}Fe^{3+}_{HS}]_{OCT}$	5	−5	5	−4	−4	5	2	Yes
Ferrimagnetic (NMM2*) $[Fe^{3+}_{HS}Fe^{3+}_{HS}]_{TET}[-Fe^{3+}_{HS} - Fe^{2+}_{HS} - Fe^{2+}_{HS}Fe^{3+}_{HS}]_{OCT}$	5	5	−5	−4	−4	5	2	Yes
Ferrimagnetic (NMM8) $[Fe^{3+}_{HS}Fe^{3+}_{HS}]_{TET}[-Fe^{3+}_{HS}Fe^{2+}_{HS}Fe^{2+}_{HS} - Fe^{3+}_{HS}]_{OCT}$	5	5	−5	4	4	−5	8	Yes
Ferrimagnetic (NMM12) $[Fe^{3+}_{HS}Fe^{3+}_{HS}]_{TET}[Fe^{3+}_{HS} - Fe^{2+}_{HS} - Fe^{2+}_{HS}Fe^{3+}_{HS}]_{OCT}$	5	5	5	−4	−4	5	12	Yes
Ferrimagnetic (NMM18) $[-Fe^{3+}_{HS}Fe^{3+}_{HS}]_{TET}[Fe^{3+}_{HS}Fe^{2+}_{HS}Fe^{2+}_{HS}Fe^{3+}_{HS}]_{OCT}$	−5	5	5	4	4	5	18	Yes
Ferromagnetic (NMM28) $[Fe^{3+}_{HS}Fe^{3+}_{HS}]_{TET}[Fe^{3+}_{HS}Fe^{2+}_{HS}Fe^{2+}_{HS}Fe^{3+}_{HS}]_{OCT}$	5	5	5	4	4	5	28	Yes

B. Calculations under pressure

High-pressure behavior of magnetite (inverse spinel and normal spinel) and h-Fe_3O_4 was studied by performing fixed volume calculations. The ions were allowed to relax, but cell shape and volume were fixed—this corresponds to ISIF = 2 in the VASP INCAR file.[29] In the magnetite 14-atom unit cell, the volume space grid was 155, 150, 145, 140, 135, 130, 125, and 120 Å^3. In the 28-atom h-Fe_3O_4 unit cell, the volume space grid was 290, 285, 280, 275, 270, 265, 260, 250, 240, 230, and 220 Å^3. For each structure and spin state, energy as a function of volume, $E(V)$, was fit to a third-order Birch–Murnaghan equation of state to determine the energy and volume as a function of pressure. From $E(P)$ and $V(P)$, enthalpy as a function of pressure, $H(P) = E(P) + P \cdot V(P)$, and the equation of state parameters were found.

C. Calculating the spin state

Our goal was to understand the spin state of Fe in Fe_3O_4. Since the spin state of Fe could be linked to site coordination (TET vs OCT), magnetic ordering, charge ordering, and charge coordination (valence), all these factors must be studied in order to have a full understanding of the spin state of Fe in Fe_3O_4. In this section, the spin calculations are laid out in detail.

To motivate the spin states studied, we first considered the spin-related changes measured as a function of pressure by Ding *et al.*, 2008. Their K-edge x-ray magnetic circular dichroism measurements showed a drop in total magnetic moment by half (a decrease of 4 to 2 μ_B/f.u., which would be 8 to 4 μ_B in our 14-atom computational unit cell), and their XES measurements showed a drop of peak intensity by ∼15%, meaning ∼15% of unpaired electrons had reduced their spins. In the formula unit of inverse-spinel magnetite (three Fe atoms) $[-Fe^{3+}]_{TET}[Fe^{3+}Fe^{2+}]_{OCT}$, there are two Fe^{3+} atoms (five unpaired electrons each, Table II) and one Fe^{2+} atom (four unpaired electrons, Table II), with a total of 14 unpaired electrons. If Fe^{2+} transitions from HS to IS (drop from four to two unpaired electrons), the reduction in unpaired electrons is 14%, consistent with measurements.[7] Another spin transition that would be consistent with measurements but not considered by Ding *et al.*, is one Fe^{3+} atom (either on the TET or OCT site, but not both) going through a HS to IS transition, corresponding to a drop in unpaired electrons by two (14%). Therefore both IS Fe^{2+} and Fe^{3+} were considered in this study. Even though transitions from HS to LS Fe^{2+} or Fe^{3+} are too high of a drop in unpaired electrons to match the experimental measurements of Ding *et al.*, these larger spin-state changes were also considered in order to map out the entire spin space (Table IV).

1. Calculating the spin state of inverse spinel

All calculations started with *Imma* symmetry (see Sec. II A), which allowed for ordering of Fe^{2+} and Fe^{3+} on the OCT sites. In VASP, the initial magnetic moments and moment directions on each Fe atom can be specified, but only the total net magnetic moment (NMM) in the 14-atom unit cell can be fixed throughout the calculation. Therefore, the direction of the moments on individual atoms can relax to different orderings as long as the NMM remains fixed. For inverse spinel, $[-Fe^{3+}_{HS} - Fe^{3+}_{HS}]_{TET}[Fe^{3+}_{HS}Fe^{2+}_{HS}Fe^{2+}_{HS}Fe^{3+}_{HS}]_{OCT}$, the net moment is 8 μ_B because the individual magnetic moments (in Bohr magnetons) are $-5 - 5 + 5 + 4 + 4 + 5$, which sum to 8 Table III.

The magnetic ordering schemes considered for HS are given in Table III. These are all possible distinct (i.e., symmetrically inequivalent) magnetic orderings in the 14-atom unit cell.

TABLE IV. Summary of all inverse-spinel magnetite spin states considered in this study, organized by site. Initial moments for each spin state and total fixed net moment for cell in the 14-atom cell. When a calculation is not *locally* metastable, the final spin state after relaxation is noted and explained in the text. Labels in () correspond to labels on Fig. 2(b).

	TET		OCT					
	Fe1	Fe2	Fe3	Fe4	Fe5	Fe6	Net moment	Locally metastable
Spin transitions on both sites								
All HS (mag1) $[-Fe^{3+}_{HS} - Fe^{3+}_{HS}]_{TET}[Fe^{3+}_{HS}Fe^{2+}_{HS}Fe^{2+}_{HS}Fe^{3+}_{HS}]_{OCT}$	−5	−5	5	4	4	5	8	Yes
All IS $[-Fe^{3+}_{IS} - Fe^{3+}_{IS}]_{TET}[Fe^{3+}_{IS}Fe^{2+}_{IS}Fe^{2+}_{IS}Fe^{3+}_{IS}]_{OCT}$	−3	−3	3	2	2	3	4	No → IS 2 + OCT
All LS $[-Fe^{3+}_{LS} - Fe^{3+}_{LS}]_{TET}[Fe^{3+}_{LS}Fe^{2+}_{LS}Fe^{2+}_{LS}Fe^{3+}_{LS}]_{OCT}$	−1	−1	1	0	0	1	0	No → LS 2 + OCT
Tetrahedral (TET) site spin transitions								
IS Fe^{3+} $[-Fe^{3+}_{IS} - Fe^{3+}_{IS}]_{TET}[Fe^{3+}_{HS}Fe^{2+}_{HS}Fe^{2+}_{HS}Fe^{3+}_{HS}]_{OCT}$	−3	−3	5	4	4	5	12	No → normal spinel HS TET, OCT
LS Fe^{3+} $[-Fe^{3+}_{LS} - Fe^{3+}_{LS}]_{TET}[Fe^{3+}_{HS}Fe^{2+}_{HS}Fe^{2+}_{HS}Fe^{3+}_{HS}]_{OCT}$	−1	−1	5	4	4	5	16	No → normal spinel IS 2+TET
OCT site spin transitions								
IS Fe^{2+} (IS 2 + OCT) $[-Fe^{3+}_{HS} - Fe^{3+}_{HS}]_{TET}[Fe^{3+}_{HS}Fe^{2+}_{IS}Fe^{2+}_{IS}Fe^{3+}_{HS}]_{OCT}$	−5	−5	5	2	2	5	4	Yes
IS Fe^{3+} $[-Fe^{3+}_{HS} - Fe^{3+}_{HS}]_{TET}[Fe^{3+}_{IS}Fe^{2+}_{HS}Fe^{2+}_{HS}Fe^{3+}_{IS}]_{OCT}$	−5	−5	3	4	4	3	4	Low pressure only → IS 2 + OCT
LS Fe^{2+} (LS 2 + OCT) $[-Fe^{3+}_{HS} - Fe^{3+}_{HS}]_{TET}[Fe^{3+}_{HS}Fe^{2+}_{LS}Fe^{2+}_{LS}Fe^{3+}_{HS}]_{OCT}$	−5	−5	5	0	0	5	0	Yes
LS Fe^{3+} $[-Fe^{3+}_{HS} - Fe^{3+}_{HS}]_{TET}[Fe^{3+}_{LS}Fe^{2+}_{HS}Fe^{2+}_{HS}Fe^{3+}_{LS}]_{OCT}$	−5	−5	1	4	4	1	0	No → LS 2 + OCT

Besides the ferromagnetic arrangement, all magnetic orderings are ferrimagnetic, except one with a net moment of 0, which is antiferromagnetic.

Energies for all these magnetic orderings as a function of pressure were calculated and the results are discussed in Sec III A. The most stable magnetic ordering $[-Fe^{3+}_{HS}-Fe^{3+}_{HS}]_{TET}[Fe^{3+}_{HS}Fe^{2+}_{HS}Fe^{2+}_{HS}Fe^{3+}_{HS}]_{OCT}$ (mag1) was used as the starting configuration for all spin-transition calculations. The atomic positions and individual moments were then allowed to relax. There are two measures of spin stability. The first measure is individual moments for a fixed NMM must retain their starting spin state after relaxation. If the spin state on the individual Fe atoms relaxes to different moments for a given initial NMM, the initial spin arrangement is not stable. If the individual spin states are the same after relaxation, then the spin state is considered *locally* stable. For each locally stable spin state, we explored a second measure to determine if the spin state is stable *globally*. Global stability is determined by plotting the enthalpy curves for different spin states as a function of pressure and determining the most stable spin state of all the spin arrangements considered at each pressure.

In the 14-atom computational cell (six Fe atoms), the HS inverse-spinel magnetite has a net moment of eight. Calculations with all IS (net moment of four) were not locally stable; the cell relaxed to HS Fe^{3+} on the TET and OCT sites and IS Fe^{2+} on the OCT (net moment of four). Calculations with all LS (net moment of zero) were also not locally stable. The cell relaxed to HS Fe^{3+} on the TET and OCT and LS Fe^{2+} on the OCT (net moment of zero). Decreasing the moment of Fe^{3+} on TET without reducing the moment on the OCT increased the total net moment (12 for IS Fe^{3+}, 16 for LS Fe^{3+}) and was not locally stable (Table IV). IS Fe^{3+} on TET relaxed to all HS normal spinel ($[-Fe^{2+}_{HS} - Fe^{2+}_{HS}]_{TET}[Fe^{3+}_{HS}Fe^{3+}_{HS}Fe^{3+}_{HS}Fe^{3+}_{HS}]_{OCT}$). LS Fe^{3+} on TET relaxed to normal spinel with IS Fe^{2+} on the TET site ($[-Fe^{2+}_{IS} - Fe^{2+}_{IS}]_{TET}[Fe^{3+}_{HS}Fe^{3+}_{HS}Fe^{3+}_{HS}Fe^{3+}_{HS}]_{OCT}$).

Unlike spin transitions on the TET site, decreasing the moment of Fe^{2+} or Fe^{3+} on the OCT site decreased the total net moment (four for IS Fe^{2+} and Fe^{3+}; zero for LS Fe^{2+} and Fe^{3+}). Magnetite with IS Fe^{3+} on the OCT site had the same total NMM as magnetite with Fe^{2+} on the OCT site. During relaxation, IS Fe^{3+} was only locally stable in the calculation for very low pressures and never globally more stable than HS. For higher pressures, Fe^{3+} on the OCT site changed to HS and Fe^{2+} relaxed to IS. For a total net moment of four, it was more energetically favorable for Fe^{2+} to change from HS to IS than for Fe^{3+}. Likewise, LS Fe^{3+} was not stable in the calculation. For a fixed total moment of zero, the calculations relaxed to LS Fe^{2+} instead of Fe^{3+}, suggesting Fe^{3+} in inverse-spinel magnetite is only stable as HS.

2. *Calculating the spin state of normal spinel*

Since there may be an inverse-spinel to normal-spinel transition in magnetite, spin transition calculations were also conducted in the normal spinel structure as a function of pressure (as will be seen in Fig. 3). All possible spin states (HS, IS, LS) on the TET and OCT sites were explored (Table V).

TABLE V. Spin states considered in the 14-atom normal-spinel magnetite unit cell. If a given spin or magnetic arrangement is not locally metastable, the final spin state after relaxation is noted and explained in the text. Labels in () correspond to labels on Fig. 3.

	TET		OCT					
	Fe1	Fe2	Fe3	Fe4	Fe5	Fe6	Net moment	Locally metastable
Spin transitions on both sites								
All HS (HS TET, OCT) $[-Fe^{2+}_{HS} - Fe^{2+}_{HS}]_{TET}[Fe^{3+}_{HS}Fe^{3+}_{HS}Fe^{3+}_{HS}Fe^{3+}_{HS}]_{OCT}$	−4	−4	5	5	5	5	12	Yes
All IS $[-Fe^{2+}_{IS} - Fe^{2+}_{IS}]_{TET}[Fe^{3+}_{IS}Fe^{3+}_{IS}Fe^{3+}_{IS}Fe^{3+}_{IS}]_{OCT}$	−2	−2	3	3	3	3	8	No → mag1
All LS $[-Fe^{2+}_{LS} - Fe^{2+}_{LS}]_{TET}[Fe^{3+}_{LS}Fe^{3+}_{LS}Fe^{3+}_{LS}Fe^{3+}_{LS}]_{OCT}$	0	0	1	1	1	1	4	No → reduced moments
TET site spin transitions								
IS Fe^{2+} (IS 2 + TET) $[-Fe^{2+}_{IS} - Fe^{2+}_{IS}]_{TET}[Fe^{3+}_{HS}Fe^{3+}_{HS}Fe^{3+}_{HS}Fe^{3+}_{HS}]_{OCT}$	−2	−2	5	5	5	5	16	Yes
LS Fe^{2+} (LS 2 + TET) $[-Fe^{2+}_{LS} - Fe^{2+}_{LS}]_{TET}[Fe^{3+}_{HS}Fe^{3+}_{HS}Fe^{3+}_{HS}Fe^{3+}_{HS}]_{OCT}$	0	0	5	5	5	5	20	Yes
OCT site spin transitions								
IS Fe^{3+} $[-Fe^{2+}_{HS} - Fe^{2+}_{HS}]_{TET}[Fe^{3+}_{IS}Fe^{3+}_{IS}Fe^{3+}_{IS}Fe^{3+}_{IS}]_{OCT}$	−4	−4	3	3	3	3	4	No → inverse spinel with reduced moments on OCT
LS Fe^{3+} $[-Fe^{2+}_{HS} - Fe^{2+}_{HS}]_{TET}[Fe^{3+}_{LS}Fe^{3+}_{LS}Fe^{3+}_{LS}Fe^{3+}_{LS}]_{OCT}$	−4	−4	1	1	1	1	-4	No → inverse spinel with reduced moments on OCT

A number of the normal spinel spin configuration calculations were not locally stable. Calculations of all IS Fe relaxed to inverse-spinel HS. Calculations of all LS Fe relaxed to Fe with moments slightly reduced from HS, maintaining a net moment of four. Reducing the spin of Fe^{3+} to LS or IS on the OCT site was not energetically favorable. To maintain the net magnetic moment, the system preferred to change the TET site to HS Fe^{3+} (inverse spinel) and reduce the total moment on every Fe atom on the OCT site.

3. *Calculating the spin state of h-Fe_3O_4*

The correct magnetic ordering also needed to be determined in the high-pressure phase, *h*-Fe_3O_4. The experimentally determined *h*-Fe_3O_4 unit cell is twice that of magnetite; therefore, spins and magnetic ordering are given for the 12 Fe atoms in the unit cell (out of 28 total atoms). Only magnetic orderings that fit within the crystallographic unit cell were considered (Table VI). Trying every possible magnetic arrangement in the 28-atom cell would be computationally impractical. Therefore, only a few representative magnetic orderings were chosen based on the results in magnetite (Fig. 2): the same magnetic ordering as magnetite, a NMM of zero, and ferromagnetic. Energetics and details of the different magnetic arrangements for *h*-Fe_3O_4 are discussed in Sec. III C.

Calculations starting with all IS or all LS Fe on the OCT and TET sites were not locally stable and relaxed to a combination of HS, LS, and reduced-spin Fe^{2+} and Fe^{3+} with a net moment of 16 (eight for all LS). Calculations that started with IS Fe^{3+} on the OCT site were not locally stable and relaxed to a combination of HS and LS Fe atoms and the TET site became Fe^{2+}.

III. RESULTS

This section is organized as follows. First, magnetic ordering and spin transitions in inverse-spinel magnetite are presented (Sec. III A). Then, results on magnetic ordering and spin transitions in normal-spinel magnetite are given (Sec. III B). The stable magnetic ordering and spin states in *h*-Fe_3O_4 are presented in Sec. III C. Section III D discusses the impact of magnetic order, spin, and normal and inverse spinel on the pressure-induced phase transition of inverse spinel magnetite to *h*-Fe_3O_4. Finally, Sec. III E gives the equations of state of the key phases as a function of pressure.

A. Magnetic ordering and spin transitions in inverse-spinel magnetite

The strong magnetic moment in inverse-spinel magnetite occurs due to ferrimagnetic $[-Fe^{3+}_{HS} - Fe^{3+}_{HS}]_{TET}[Fe^{3+}_{HS}Fe^{2+}_{HS}Fe^{2+}_{HS}Fe^{3+}_{HS}]_{OCT}$ ordering between the TET and OCT sites.[14] We tested that this is the correct magnetic ordering in inverse-spinel magnetite by comparing the enthalpies as a function of pressure for multiple magnetic arrangements in the charge-ordered structure. The relative enthalpies of the different magnetic orderings are plotted in Fig. 2(a). The figure clearly shows that ferrimagnetic ordering between the TET and OCT sites $[-Fe^{3+}_{HS} - Fe^{3+}_{HS}]_{TET}[Fe^{3+}_{HS}Fe^{2+}_{HS}Fe^{2+}_{HS}Fe^{3+}_{HS}]_{OCT}$ (mag1) is the most stable for all pressures by more than 140 meV/f.u. and is used for the remainder of the inverse-spinel magnetite spin studies. There is no magnetic ordering transition under pressure in magnetite. Ferrimagnetic ordering (FM) is over 0.8 eV/f.u., less stable than ferromagnetic mag1.

TABLE VI. Magnetic orderings and spin arrangements considered in 28-atom h-Fe_3O_4. To conserve space, individual moments are not listed. When a calculation is not locally stable, the final spin state after relaxation is noted and explained in the text. Labels in () correspond to labels on Fig. 4.

	Net moment	Locally metastable
Magnetic ordering arrangements, all HS		
Inverse spinel, ferrimagnetic (mag1)		
$[-Fe^{3+}_{HS} - Fe^{3+}_{HS} - Fe^{3+}_{HS} - Fe^{3+}_{HS}]_{TET}[Fe^{3+}_{HS}Fe^{3+}_{HS}Fe^{2+}_{HS}Fe^{2+}_{HS}Fe^{2+}_{HS}Fe^{2+}_{HS}Fe^{3+}_{HS}Fe^{3+}_{HS}]_{OCT}$	16	Yes
h-Fe_3O_4, antiferromagnetic (h-NMM0)		
$[Fe^{2+}_{HS} - Fe^{2+}_{HS}Fe^{2+}_{HS} - Fe^{2+}_{HS}]_{TET}[Fe^{3+}_{HS} - Fe^{3+}_{HS}Fe^{3+}_{HS} - Fe^{3+}_{HS}Fe^{3+}_{HS} - Fe^{3+}_{HS}Fe^{3+}_{HS} - Fe^{3+}_{HS}]_{OCT}$	0	Yes
h-Fe_3O_4, ferrimagnetic (h-NMM24)		
$[-Fe^{2+}_{HS} - Fe^{2+}_{HS} - Fe^{2+}_{HS} - Fe^{2+}_{HS}]_{TET}[Fe^{3+}_{HS}Fe^{3+}_{HS}Fe^{3+}_{HS}Fe^{3+}_{HS}Fe^{3+}_{HS}Fe^{3+}_{HS}Fe^{3+}_{HS}Fe^{3+}_{HS}]_{OCT}$	24	Yes
h-Fe_3O_4, ferromagnetic (h-FM)		
$[Fe^{2+}_{HS}Fe^{2+}_{HS}Fe^{2+}_{HS}Fe^{2+}_{HS}]_{TET}[Fe^{3+}_{HS}Fe^{3+}_{HS}Fe^{3+}_{HS}Fe^{3+}_{HS}Fe^{3+}_{HS}Fe^{3+}_{HS}Fe^{3+}_{HS}Fe^{3+}_{HS}]_{OCT}$	56	Yes
Spin transitions on both sites		
All IS		
$[-Fe^{2+}_{IS} - Fe^{2+}_{IS} - Fe^{2+}_{IS} - Fe^{2+}_{IS}]_{TET}[Fe^{3+}_{IS}Fe^{3+}_{IS}Fe^{3+}_{IS}Fe^{3+}_{IS}Fe^{3+}_{IS}Fe^{3+}_{IS}Fe^{3+}_{IS}Fe^{3+}_{IS}]_{OCT}$	16	No → reduced moments
All LS		
$[-Fe^{2+}_{LS} - Fe^{2+}_{LS} - Fe^{2+}_{LS} - Fe^{2+}_{LS}]_{TET}[Fe^{3+}_{LS}Fe^{3+}_{LS}Fe^{3+}_{LS}Fe^{3+}_{LS}Fe^{3+}_{LS}Fe^{3+}_{LS}Fe^{3+}_{LS}Fe^{3+}_{LS}]_{OCT}$	8	No → reduced moments
TET site spin transitions		
IS Fe^{2+} (IS 2 + TET)		
$[-Fe^{2+}_{IS} - Fe^{2+}_{IS} - Fe^{2+}_{IS} - Fe^{2+}_{IS}]_{TET}[Fe^{3+}_{HS}Fe^{3+}_{HS}Fe^{3+}_{HS}Fe^{3+}_{HS}Fe^{3+}_{HS}Fe^{3+}_{HS}Fe^{3+}_{HS}Fe^{3+}_{HS}]_{OCT}$	32	Yes
LS Fe^{2+} (LS 2 + TET)		
$[-Fe^{2+}_{LS} - Fe^{2+}_{LS} - Fe^{2+}_{LS} - Fe^{2+}_{LS}]_{TET}[Fe^{3+}_{HS}Fe^{3+}_{HS}Fe^{3+}_{HS}Fe^{3+}_{HS}Fe^{3+}_{HS}Fe^{3+}_{HS}Fe^{3+}_{HS}Fe^{3+}_{HS}]_{OCT}$	40	Yes
OCT site spin transitions		
IS Fe^{3+}		
$[-Fe^{2+}_{HS} - Fe^{2+}_{HS} - Fe^{2+}_{HS} - Fe^{2+}_{HS}]_{TET}[Fe^{3+}_{IS}Fe^{3+}_{IS}Fe^{3+}_{IS}Fe^{3+}_{IS}Fe^{3+}_{IS}Fe^{3+}_{IS}Fe^{3+}_{IS}Fe^{3+}_{IS}]_{OCT}$	8	No → reduced moments
LS Fe^{3+}, ferromagnetic (LS 3 + OCT)		
$[Fe^{2+}_{HS}Fe^{2+}_{HS}Fe^{2+}_{HS}Fe^{2+}_{HS}]_{TET}[Fe^{3+}_{LS}Fe^{3+}_{LS}Fe^{3+}_{LS}Fe^{3+}_{LS}Fe^{3+}_{LS}Fe^{3+}_{LS}Fe^{3+}_{LS}Fe^{3+}_{LS}]_{OCT}$	24	Yes
LS Fe^{3+}, ferromagnetic (LS 3 + OCT)		
$[-Fe^{2+}_{HS} - Fe^{2+}_{HS} - Fe^{2+}_{HS} - Fe^{2+}_{HS}]_{TET}[Fe^{3+}_{LS}Fe^{3+}_{LS}Fe^{3+}_{LS}Fe^{3+}_{LS}Fe^{3+}_{LS}Fe^{3+}_{LS}Fe^{3+}_{LS}Fe^{3+}_{LS}]_{OCT}$	−8	Yes

The spin transition pressure of Fe is considered on both TET and OCT sites [Fig. 2(b)]. Table IV lists the spin states considered, the initial individual moments specified on each atom, and the total magnetic moment. Fe^{3+} on the TET site in inverse-spinel magnetite remains HS for all pressures. Neither all IS nor LS Fe on the TET site are locally stable in the calculations (Table IV).

The relative enthalpies of HS, IS, and LS Fe^{2+} on the OCT site are plotted in Fig. 2(b). IS Fe^{2+} is 1 eV/f.u. less stable at ambient pressure than HS Fe. LS Fe^{2+} is 1.2 eV/f.u. less stable than HS. For all pressures up to 45 GPa (the highest considered), Fe^{2+} and Fe^{3+} in inverse-spinel magnetite will remain HS. To be sure that the instability of the IS state was not due to our specific value of U, a range of U values were explored. Increasing U, stabilizes HS magnetite with respect to IS and decreases the h-Fe_3O_4 to magnetite phase transition pressure.[29]

The experimentally observed phases involve unit cells significantly larger than the 14-atom unit cell. Pursuing larger cells with more complex charge ordering would greatly complicate and slow the calculations. In fact, in addition to the 14-atom charge-ordered structure with *Imma* symmetry, the 56-atom structure charge-ordered structure with $P2/c$ monoclinic symmetry (*Pmca* pseudosymmetry)[27] was also used. The larger unit cell was calculated with IS Fe^{2+} on the OCT site. IS was not metastable in the calculations; the Fe spins relaxed to a mixture of HS and LS Fe^{2+} and Fe^{3+}. In VASP, only the total moment can be fixed; moments on individual atoms cannot be fixed. The larger unit cell made controlling the individual spins on the Fe atoms computationally impossible; therefore, the simpler *Imma* symmetry was chosen for easier control of Fe's spin state.

B. Magnetic ordering and spin transitions in normal spinel magnetite

Normal spinel is less stable than inverse spinel (mag1) by over 0.77 eV/f.u. for all pressures (Fig. 3). As in the case of inverse spinel, IS and LS Fe^{2+} on the TET site in normal spinel are energetically unfavorable with respect to HS iron. Spin transitions on the OCT site were considered (Table V), especially IS Fe^{3+}, which has a net moment of four. However, changing to IS on the OCT site was not locally stable, and upon relaxation the system formed inverse spinel (Fe^{3+} on the TET site) and reduced the moment of Fe^{2+} on the OCT site (without actually flipping an electron spin to fully form the IS state).

C. Magnetic ordering and spin states in h-Fe_3O_4

The most stable magnetic ordering in h-Fe_3O_4 is antiferromagnetic ordering (h-NMM0) with a total net moment of zero [Fig. 4(a)]. Ferrimagnetic ordering between TET and OCT (h-NMM24) with a net moment of 24 has very

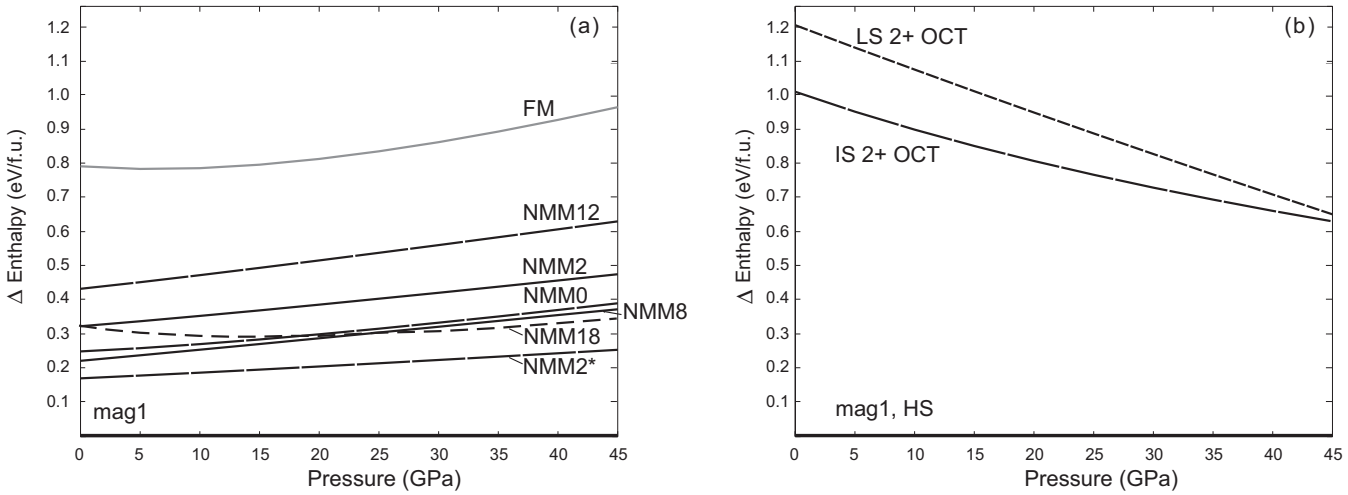

FIG. 2. (a) Stable magnetic ordering in inverse-spinel magnetite. All enthalpies are referenced to HS magnetite, mag1. (b) Spin states in inverse-spinel magnetite. Enthalpies of Fe^{2+} in HS, IS, and (LS) states on the OCT site referenced to HS magnetite.

similar energetics to the antiferromagnetic ordering, differing by ∼20 meV/f.u.. There is an approximately 140 meV/f.u. difference between ferrimagnetic and FM in h-Fe_3O_4.

IS Fe^{2+} on the TET site is more than 0.84 eV/f.u. less stable than HS [Fig. 4(b)]. LS Fe^{2+} on the TET site is more than 1.26 eV/f.u. less stable than HS Fe^{2+}. Ferrimagnetic LS Fe^{3+} on the OCT site and ferromagnetic Fe^{3+} on the OCT site have similar enthalpies (to within 140 meV/f.u.), but both are more than 2.1 eV/f.u. less stable than HS h-Fe_3O_4. Therefore, HS Fe remains stable in both TET and OCT sites for all pressures considered in this study (up to 45 GPa).

It is worth noting that in both magnetite and h-Fe_3O_4, spin lowering in Fe^{2+} was more stable than spin lowering in Fe^{3+}. If the initial moments were set such that Fe^{3+} had a lower moment, the relaxations tended to favor flipping the spin on the Fe^{2+} rather than on the Fe^{3+}. This demonstrates a clear coupling of valence and spin state, with Fe^{3+} favoring HS more than Fe^{2+} in the magnetite structure. This result might be expected due to the half-filled d-shell providing additional stabilization in the Fe^{3+} HS state.

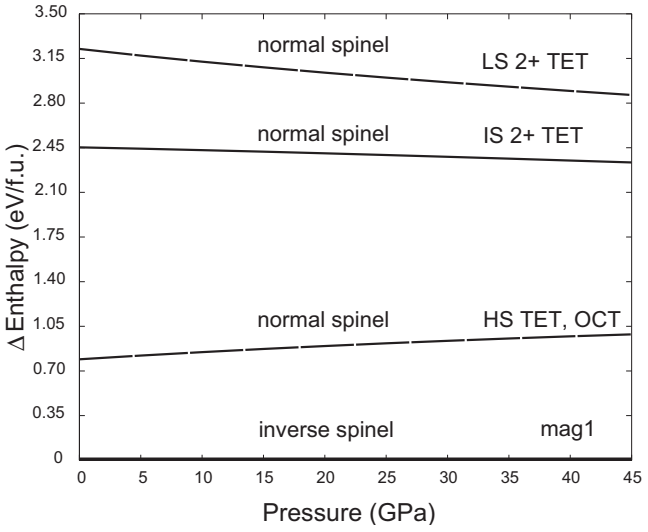

FIG. 3. Stable spin states in normal-spinel magnetite. All enthalpies are referenced to HS magnetite with the inverse-spinel structure, mag1. Details of the magnetic arrangements can be found in Table V.

D. Phase transitions under pressure: inverse-spinel magnetite to h-Fe_3O_4 structure

Based on the most stable spin states vs pressure for inverse-spinel magnetite, normal-spinel magnetite, and h-Fe_3O_4 there is a predicted phase transition from the inverse-spinel magnetite to h-Fe_3O_4 at 10 GPa. Below 10 GPa the most stable state is the inverse-spinel magnetite structure (mag1) with HS Fe and ferrimagnetic ordering between the OCT and TET sites (Fig. 4). Above 10 GPa, the most stable state is the normal-spinel high-pressure magnetite structure h-Fe_3O_4 with HS Fe. This corresponds to an inverse-spinel to normal-spinel transition due to the phase transition. Within magnetite (mag1), there is no inverse- to normal-spinel transition. The proposed inverse $[Fe^{3+}]_{TET}[Fe^{2+/3+}Fe^{2+/3+}]_{OCT}$ to normal $[Fe^{2+}]_{TET}[Fe^{3+}Fe^{3+}]_{OCT}$ spinel transition in magnetite around 8–15 GPa[15,16] was not supported by the calculations (Fig. 3). As illustrated in the previous figures, there are no spin transitions in inverse-spinel or normal-spinel magnetite or h-Fe_3O_4 as a function of pressure. Across the phase transition, the volume decreases by 7% to 8%, consistent with experimentally measured volume changes (Fig. 5). In magnetite, the calculated volume is almost 4% higher than the experimental values at all pressures (Fig. 5). The discrepancy is consistent with typical volume overestimation of a few percent between GGA simulations and the experiment. However, some of the error may come from comparing the *Imma* structure of this study, which has charge ordering on the OCT site, with the $Fd\bar{3}m$ structure,[17] which is charge averaged. The ordering on the OCT site of *Imma* may expand the lattice relative to the charge-averaged structure ($Fd\bar{3}m$). In h-Fe_3O_4, the computational volume is less than 3% larger than the experimental volume (Fig. 5), also consistent with GGA simulations, overestimation of the volume. A full structural

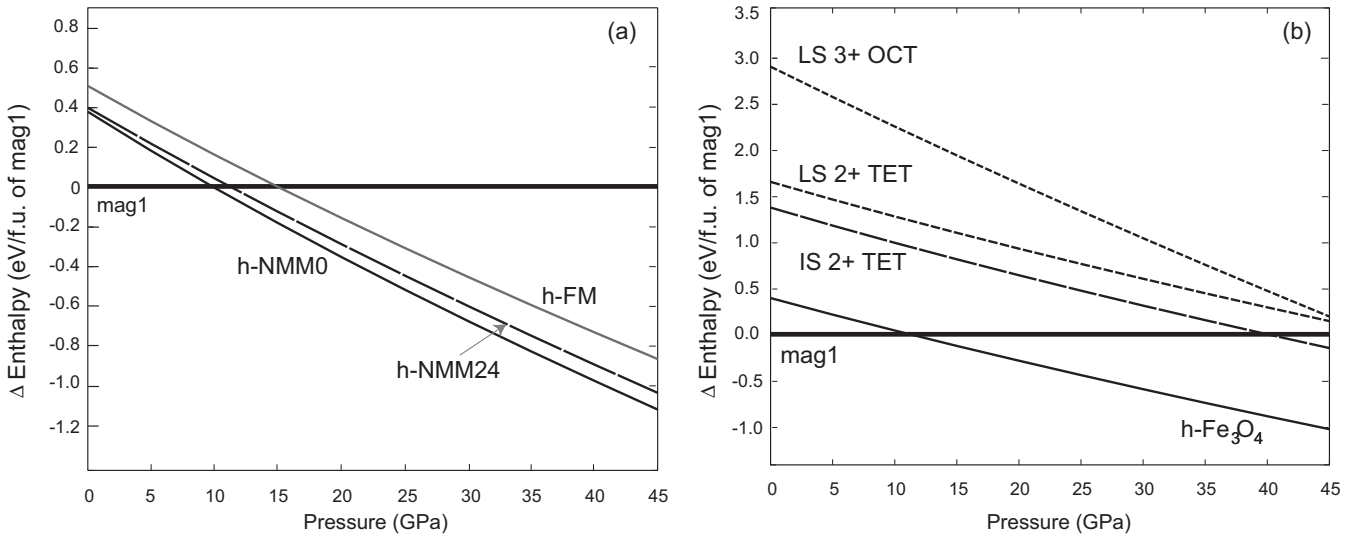

FIG. 4. (a) Stable magnetic arrangements in normal spinel h-Fe_3O_4 referenced to HS magnetite, mag1. (b) Stable spin states in h-Fe_3O_4 *Pbcm*.

comparison between this study and literature values is given in the Supplemental Material.[29]

The system also undergoes an insulating to metal transition, which can be seen in the electronic density of states (DOS) shown in Fig. 6. Magnetite (charge ordered, *Imma*) is insulating at the ground state with a band gap of just under 0.2 eV at 0 GPa, consistent with previous computational and experimental studies.[30] Magnetite remains insulating up to 21 GPa. However h-Fe_3O_4 exhibits metallic behavior, with a significant DOS at the Fermi level at 20 GPa.

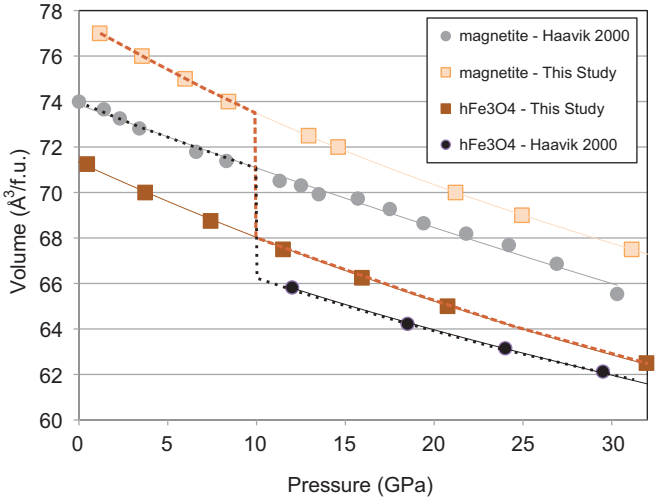

FIG. 5. (Color online) Volume change across the phase transition from inverse-spinel magnetite ($[-Fe^{3+}_{HS} - Fe^{3+}_{HS}]_{TET}[Fe^{3+}_{HS}Fe^{2+}_{HS}Fe^{2+}_{HS}Fe^{3+}_{HS}]_{OCT}$) to h-Fe_3O_4 ($[-Fe^{2+}]_{TET}[Fe^{3+}Fe^{3+}]_{OCT}$). The volume curves for each phase are given in orange squares (light for magnetite, dark for h-Fe_3O_4). The dashed orange line follows the stable phase as a function of pressure. Experimental volumes for magnetite and h-Fe_3O_4 (gray/black circles; Ref. 17) are shown for comparison with the calculations. The dashed black line follows the experimental stable phase as a function of pressure.

E. Bulk elastic properties as a function of pressure

The equation of state parameters were calculated for Fe_3O_4 (Table VII). The calculated bulk modulus, B_0, of inverse- and normal-spinel magnetite vary by less than 5 GPa and are more compressible than h-Fe_3O_4 by over 15 GPa. Likewise, the volumes of inverse and normal spinel are similar to each other and larger than V_0 of h-Fe_3O_4 by almost 0.9 Å^3/atom. For all cases, lowering the spin state from HS to IS and LS raises E_0 and lowers V_0. B' remains almost unchanged for lower spin states. In magnetite, B_0 and B' are in the same range as other experimental and computational values (Table VII). As explained previously, the calculated V_0 is ~4% larger than the one obtained from experiments.

IV. DISCUSSION

The calculations of the magnetic ordering in inverse spinel magnetite indicate that there is ferrimagnetic ordering between the TET and OCT sites with a residual moment of 8 μ_B/14-atom unit cell (4 μ_B/f.u.). All possible magnetic ordering arrangements in the 14-atom cell were calculated. We confirmed that the inverse-spinel ordering, $[-Fe^{3+}_{HS} - Fe^{3+}_{HS}]_{TET}[Fe^{3+}_{HS}Fe^{2+}_{HS}Fe^{2+}_{HS}Fe^{3+}_{HS}]_{OCT}$, is still the most stable magnetic ordering configuration up to 45 GPa. The computational results, therefore, suggest that the reduction of total moment by one half observed experimentally[7] cannot be attributed to a change of magnetic ordering arrangements.

Having the correct magnetic arrangement at ambient pressure allowed for studying the spin in the correct structure. In our study, we accounted for Fe in different sites (TET and OCT), Fe with different valence (Fe^{2+} and Fe^{3+}), and different charge coordination (inverse spinel and normal spinel). Iron remained high spin for all charge sets, site occupations, pressures, and structures considered. In the calculations, there is no pressure-induced transition from inverse-spinel magnetite to normal-spinel magnetite. The calculations predict a pressure-induced phase transition from inverse-spinel magnetite to normal-spinel h-Fe_3O_4 at 10 GPa, in agreement with some older experimental measurements[17–19]

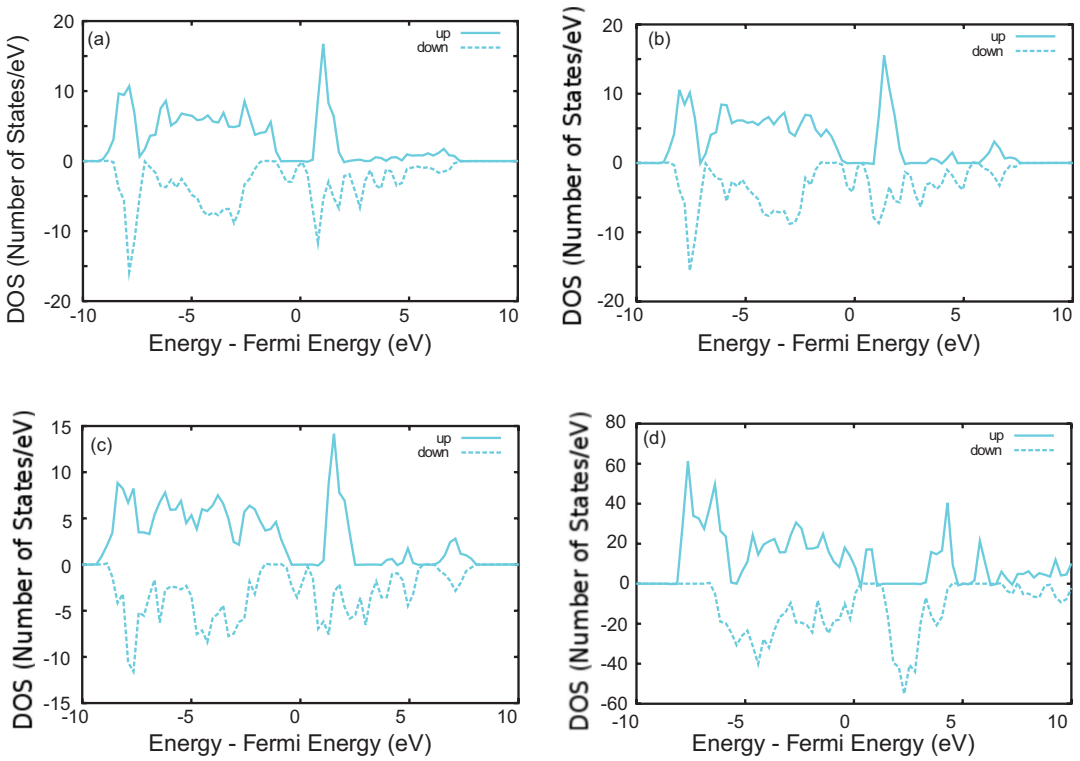

FIG. 6. (Color online) Electronic structure of (a) magnetite, $[-Fe^{3+}_{HS} - Fe^{3+}_{HS}]_{TET}[Fe^{3+}_{HS}Fe^{2+}_{HS}Fe^{2+}_{HS}Fe^{3+}_{HS}]_{OCT}$, at ambient pressure (b) magnetite at 1 GPa, (c) magnetite at 21.1 GPa, and (d) *h*-Fe3O4, $[-Fe^{2+}]_{TET}[Fe^{3+}Fe^{3+}]_{OCT}$, at 20.8 GPa with HS Fe on all sites. The Fermi energy has been subtracted from all energy values. The density of states (DOS) is reported as the number of states per electron volt in the unit cell.

but contradictory to more recent experiments.[4,20] Instead of finding a phase transition, Baudelet *et al.* (2010) and Glazyrin *et al.* (2012) found the magnetic moment decreases with increasing pressure.

The high-pressure *h*-Fe_3O_4 phase is predicted to be antiferromagnetic, but the enthalpies of all magnetic ordering arrangements considered are within 0.175 eV/f.u. of each other. The close energetics are in contrast with inverse-spinel magnetite where magnetic orderings vary by over 0.875 eV/f.u. Therefore, magnetic ordering has a much greater stabilizing effect in inverse-spinel magnetite than in *h*-Fe_3O_4. The small energy difference between different magnetic arrangements in *h*-Fe_3O_4 may explain why it has been measured as being paramagnetic at room temperature.[17] The *h*-Fe_3O_4 phase also remains HS for pressures up to 45 GPa (the highest of this study). Therefore, the calculations predict that Fe_3O_4 will undergo a phase transition at 10 GPa, but the spin state of Fe will remain HS for all pressures.

DFT calculations are effectively at absolute zero and therefore do not include temperature effects. From the DFT

TABLE VII. Equation of state parameters for Fe_3O_4 at ambient pressure. Energy, E_0, bulk modulus, B_0, the pressure derivative of the bulk modulus, B', and the ground state volume, V_0, come from fits to a third-order Birch–Murnaghan equation of state. Parameters are given for HS, IS, and LS Fe.

	Magnetite: inverse spinel				*h*-Fe_3O_4		
	HS	Literature (HS)	IS 2 + OCT	LS 2 + OCT	HS	IS 2 + TET	LS
E_0 (eV/atom)	−6.946		−6.802	−6.774	−6.888	−6.751	–
B_0 (GPa)	173	141 − 222,[17] 180.6[16]	188	172	189	187	–
B'	3.97	4 − 7.5,[17] 4.33[16]	3.98	3.92	4.02	4.00	–
V_0 (Å^3/atom)	11.07	10.57[16]	10.78	10.76	10.19	10.15	–
	Magnetite: normal spinel						
	HS	IS 2 + TET	LS 2 + TET				
E_0 (eV/atom)	−6.833	−6.596	–				
B_0 (GPa)	169	170	–				
B'	3.83	3.89	–				
V_0 (Å^3/atom)	11.21	11.02	–				

TABLE VIII. The magnitudes of the magnetic, $T\Sigma_{\text{magnetic}} = kT\ln(2S+1)$, and electronic, $T\Sigma_{\text{electronic}} = kT\ln(D)$, entropy contributions to the free energy for HS ($3t_{2g}\uparrow 2e_g\uparrow t_{2g}\downarrow$), IS ($3t_{2g}\uparrow 1e_g\uparrow 2t_{2g}\downarrow$), and LS ($3t_{2g}\uparrow 3t_{2g}\downarrow$) Fe^{2+}. S_σ is the spin number, and D is the electron degeneracy in t_{2g} and e_g. At room temperature, kT is approximately 0.026 eV. There are three Fe atoms in a formula unit of Fe_3O_4; therefore, $\Sigma_{\text{magnetic}}+\Sigma_{\text{electronic}}$ is reported for three Fe atoms. The expression for Σ_{magnetic} above is only applicable to paramagnets. If magnetite (HS Fe) has strong magnetic ordering, there will be no magnetic entropy term ($T\Sigma_{\text{magnetic}}=0$). We assume the other phases are paramagnetic. Assuming magnetite with IS Fe is paramagnetic provides an upper bound on its free-energy gain associated with the magnetic degrees of freedom. The total contribution to the free energy is given by $-T\Sigma_{\text{total}}$.

	S_σ	D	(kT/f.u.)	$T\Sigma_{\text{magnetic}}$ (kT/f.u.)	$T\Sigma_{\text{electronic}}$ (kT/f.u.)	$T\Sigma_{\text{total}} = T\Sigma_{\text{magnetic}} + T\Sigma_{\text{electronic}}$ (eV/f.u. at room temperature)	$-T\Sigma_{\text{total}}$
HS	2	3 t_{2g}	Magnetite (magnetically ordered)	0	$3kT\ln(3)$	$3kT\ln(3)$	−0.086
			Magnetite (paramagnetic)	$3kT\ln(5)$	$3kT\ln(3)$	$3kT(\ln(15))$	−0.211
			h-Fe_3O_4	$3kT\ln(5)$	$3kT\ln(3)$	$3kT(\ln(15))$	−0.211
IS	1	3 t_{2g}, 2 e_g (total= $3\times 2=6$)	Magnetite	$3kT\ln(3)$	$3kT\ln(6)$	$3kT(\ln(18))$	−0.225
			h-Fe_3O_4	$3kT\ln(3)$	$3kT\ln(6)$	$3kT(\ln(18))$	−0.225
LS	0	1 t_{2g}	Magnetite	$3kT\ln(1)$	$3kT\ln(1)$	0	−0.000
			h-Fe_3O_4	$3kT\ln(1)$	$3kT\ln(1)$	0	−0.000

calculations alone, it is not clear if increasing temperature could stabilize IS with respect to HS. The effect of temperature on the spin transition can be determined from the Gibbs free-energy expression ($G = H - T\Sigma$). The Gibbs free energy is the sum of the enthalpy H and entropy Σ (vibrational, magnetic, electronic) terms multiplied by temperature T. The enthalpy was calculated from DFT (see Results section). The entropic terms relevant to spin are the magnetic and electronic entropies estimated for a paramagnetic phase as

$$\Sigma_{\text{magnetic}} = k\ln(2S_\sigma + 1),$$
$$\Sigma_{\text{electronic}} = k\ln(D),$$

where S_σ is the spin quantum number, D is the orbital degeneracy in t_{2g} and e_g states, and k is the Boltzmann constant. S_σ and D values for HS, IS, and LS Fe^{2+} and Fe^{3+} in OCT and TET sites are shown in Table VIII, where D values are estimated from crystal-field arguments.[31] The entropy contributions to the free energy in units of kT ($kT = 0.026$ eV) evaluated at room temperature are given in Table VIII. These estimates assume all phases are paramagnetic except for HS magnetite, which is known to have strong magnetic ordering at room temperature. This approach gives the largest possible temperature dependence to the free-energy estimates and therefore provides an upper bound on the magnetic and electronic contributions to the spin and phase stability. In magnetite, the sum of the magnetic and electronic contributions to the entropy are -0.086 eV/f.u. for HS Fe^{2+}, -0.225 eV/f.u. for IS Fe^{2+}, and 0 eV/f.u. for LS Fe^{2+} (at room temperature). These additional contributions to the free energy from the electronic and magnetic contributions will only reduce ΔH by 0.139 eV/f.u. at room temperature (0.463 eV/f.u. at 1000 K), which is too small to stabilize IS [Fig. 2(b)].

The effect of temperature and the electronic and spin degrees of freedom on the phase transition from magnetite to h-Fe_3O_4 [Fig. 4(b)] can also be estimated using the same arguments. At room temperature, magnetite with HS Fe^{2+} has strong magnetic ordering [Fig. 2(a)], and thus no magnetic entropy contribution; therefore, the entropic and temperature contributions to Gibbs free energy due to HS Fe^{2+} is -0.086 eV/f.u. The high-pressure phase h-Fe_3O_4 has weak magnetic ordering [Fig. 4(a); paramagnetic, Table VIII], leading to a total contribution to the Gibbs free energy of -0.211 eV/f.u. Thus, temperature will drive the phase transition toward lower pressures and reduce ΔH by 0.125 eV/f.u. (at 300 K). If h-Fe_3O_4 retains magnetic ordering, then the entropy contributions to the Gibbs free energy will be the same for magnetite and h-Fe_3O_4, and the phase transition will remain unchanged.

It should be noted that there are also vibrational contributions to the free energies of the different phases and spin states in this study. However, we assume that the change in vibrational free energy between different spin states is small due to the general similarity of the structures involved. Furthermore, we expect that lower spin states will produce smaller volumes and correspondingly stiffer lattices, which will reduce the stabilizing effects of vibrational degrees of freedom.[32] Therefore, it is expected that a rigorous treatment of vibrational contributions will only further destabilize the IS and LS states. The vibrational contributions to the magnetite to h-Fe_3O_4 transition are not clear; however, because the high-pressure phase is stiffer, it is expected to be destabilized by vibrational contributions, leading to some lowering of the phase transition pressure with increasing temperature.

Magnetite is now the third system in which experimental x-ray emission spectra measurements have been interpreted as IS Fe, but theoretical calculations have not found IS to be stable. In the other systems, $(Mg,Fe)SiO_3$ perovskite and postperovskite, XES measurements show a drop in peak intensity to a nonzero value, which is interpreted as IS.[8,33] Yet, calculations in perovskite do not predict IS Fe to be theoretically stable.[9,13,34] In magnetite, perovskite, and postperovskite, the satellite peak from the XES measurements did not completely disappear. In systems where XES measurements show a drop in satellite peak intensity to zero, good agreement exists between theory and XES measurement interpretations. For example, both theory and XES measurements support a

HS to LS transition in (Mg,Fe)O ferropericlase (see Ref. 35 and references within) and FeS.[11]

There are two implications of this experimental–theoretical discrepancy. The first is a possible a limitation in the *ab initio* methods. To test this hypothesis, two additional quantum mechanical approaches were used. DMol,[3] a DFT approach with localized basis function methods,[12] was chosen to test if the localized basis functions of DMol[3] better describe IS Fe than the plane-wave basis functions used in VASP. VASP hybrid DFT–Hartree–Fock methods[36] were also explored to see if the addition of Hartree–Fock terms to the energetics changed the qualitative predictions regarding IS. The energy of magnetite was calculated with both methods for HS, IS, and LS Fe^{2+} on the OCT site.[29] All approaches predict that the OCT Fe^{2+} will remain HS up to 40 GPa (see Table A1 in Supplemental Materials[29]). DFT using plane waves and local basis functions, as well as hybrid DFT–Hartree–Fock methods all find HS Fe to be stable with respect to IS Fe. Cluster-based DFT methods with newer functionals do not find a stable IS state in perovskite[13] and other iron-bearing complexes either.[37] The agreement among these various methods suggests the calculations are capturing the correct spin behavior of iron; however, the small possibility exists that essential physics of IS are not accurately described.

The more plausible implication of the experimental–theoretical discrepancy is that the observed drop of satellite peak intensity to a nonzero value in XES measurements at high pressure is due to a change other than a transition to IS iron, such as electron delocalization with pressure.[4,20] If XES with a satellite peak that is reduced to a nonzero value cannot be interpreted as IS Fe^{2+}, then Fe^{2+} in magnetite, perovskite, and postperovskite will remain HS.

V. CONCLUSIONS

The *ab initio* calculations isolated the complex magnetic ordering, valence states, charge ordering, and different local Fe site environments in magnetite and h-Fe_3O_4 as a function of pressure. The calculations found a pressure-induced structural phase transition from inverse-spinel magnetite to normal-spinel h-Fe_3O_4. The magnetic ordering of inverse-spinel magnetite does not change with pressure and iron remains HS for all pressures. There is no evidence from the *ab initio* energetics for an inverse-spinel to normal-spinel transition with pressure in magnetite. However, the magnetite to high-pressure magnetite h-Fe_3O_4 phase transition corresponds to an inverse-spinel to normal-spinel transition, where h-Fe_3O_4 has a different symmetry and structure from magnetite.

The most stable spin state is HS Fe in the ferrimagnetic arrangement for both magnetite and high-pressure magnetite h-Fe_3O_4 structures up to 45 GPa (the highest pressure considered in this study). The calculations have accounted for site occupation, valence, and charge coordination. IS iron is not stable in magnetite, contrary to experimental measurements.[7] The discrepancy between theoretical and experimental measurements of IS iron only occurs when the x-ray emission spectra satellite peak intensity drops to a nonzero value, which has been seen in magnetite, perovskite, and postperovskite. The results suggest x-ray emission spectra may need to be interpreted differently at high pressures. The lack of IS in magnetite implies Fe^{2+} in perovskite and postperovskite will also remain HS.

ACKNOWLEDGMENTS

The majority of this work was completed while A. Bengtson was at the University of Michigan. The authors gratefully acknowledge funding from the Turner Postdoctoral Fellowship at the University of Michigan for salary for A. Bengtson while at University of Michigan. The authors also acknowledge the National Science Foundation Geosciences directorate, Earth Sciences Research (EAR) division (Grant No. 0966899) for support of A. Bengtson and D. Morgan at University of Wisconsin. U. Becker acknowledges support from US Department of Energy DOE-SBR (Grant No. DE-SC0004883). The authors are grateful to Peter van Keken and Michael Messina for computational support and to the Computational Mineralogy Group at the University of Michigan and Jie Li for helpful discussions.

*Corresponding author: ddmorgan@wisc.edu

[1] D. J. Dunlop and O. Özdemir, *Rock Magnetism: Fundamentals and Frontiers*, 1st ed. (Cambridge University Press, Cambridge, 1997).
[2] P. E. van Keken, Earth Planet. Sci. Lett. **215**, 323 (2003).
[3] D. I. Gough, Earth-Sci. Rev. **32**, 3 (1992).
[4] K. Glazyrin, C. McCammon, L. Dubrovinsky, M. Merlini, K. Schollenbruch, A. Woodland, and M. Hanfland, Am. Mineral. **97**, 128 (2012).
[5] J. F. Lin and T. Tsuchiya, Phys. Earth Planet. Inter. **170**, 248 (2008).
[6] M. Dolg, U. Wedig, H. Stoll, and H. Preuss, J. Chem. Phys. **86**, 866 (1987).
[7] Y. Ding, D. Haskel, S. G. Ovchinnikov, Y. C. Tseng, Y. S. Orlov, J. C. Lang, and H. K. Mao, Phys. Rev. Lett. **100**, 045508 (2008).
[8] C. McCammon, I. Kantor, O. Narygina, J. Rouquette, U. Ponkratz, I. Sergueev, M. Mezouar, V. Prakapenka, and L. Dubrovinsky, Nat. Geosci. **1**, 684 (2008); Jung-Fu Lin, Heather Watson, Gyorgy Vanko, Esen E. Alp, Vitali B. Prakapenka, Przemek Dera, Viktor V. Struzhkin, Atsushi Kubo, Jiyong Zhao, Catherine McCammon, and William J. Evans, *ibid.* **1**, 688 (2008).
[9] A. Bengtson, J. Li, and D. Morgan, Geophys. Res. Lett. **36**, L15301 (2009); Han Hsu, Koichiro Umemoto, Peter Blaha, and Renata M. Wentzcovitch, Earth Planet. Sci. Lett. **294**, 19 (2010).
[10] V. I. Anisimov, F. Aryasetiawan, and A. I. Lichtenstein, J. Phys.: Condens. Matter **9**, 767 (1997).
[11] R. S. Kumar, Y. Zhang, Y. M. Xiao, J. Baker, A. Cornelius, S. Veeramalai, P. Chow, C. F. Chen, and Y. S. Zhao, Appl. Phys. Lett. **99**, 061913 (2011).
[12] B. Delley, J. Chem. Phys. **92**, 508 (1990).
[13] James R. Rustad and Qing-Zhu Yin, Nat. Geosci. **2**, 514 (2009).
[14] E. J. W. Verwey, Nature (London) **144**, 327 (1939).
[15] M. P. Pasternak, W. M. Xu, G. K. Rozenberg, R. D. Taylor, and R. Jeanloz, J. Phys. Chem. Solids **65**, 1531 (2004).

[16]G. K. Rozenberg, Y. Amiel, W. M. Xu, M. P. Pasternak, R. Jeanloz, M. Hanfland, and R. D. Taylor, Phys. Rev. B **75**, 020102 (2007).
[17]C. Haavik, S. Stolen, H. Fjellvag, M. Hanfland, and D. Hausermann, Am. Mineral. **85**, 514 (2000).
[18]Y. W. Fei, D. J. Frost, H. K. Mao, C. T. Prewitt, and D. Hausermann, Am. Mineral. **84**, 203 (1999).
[19]L. S. Dubrovinsky, N. A. Dubrovinskaia, C. McCammon, G. K. Rozenberg, R. Ahuja, J. M. Osorio-Guillen, V. Dmitriev, H. P. Weber, T. Le Bihan, and B. Johansson, J. Phys.: Condens. Matter **15**, 7697 (2003).
[20]F. Baudelet, S. Pascarelli, O. Mathon, J. P. Itie, A. Polian, and J. C. Chervin, Phys. Rev. B **82**, 140412 (2010).
[21]G. Kresse and J. Furthmuller, Comput. Mater. Sci. **6**, 15 (1996); Phys. Rev. B **54**, 11169 (1996); G. Kresse and J. Hafner, *ibid.* **47**, 558 (1993).
[22]G. Kresse and D. Joubert, Phys. Rev. B **59**, 1758 (1999); P. E. Blochl, *ibid.* **50**, 17953 (1994).
[23]J. P. Perdew, K. Burke, and M. Ernzerhof, Phys. Rev. Lett. **77**, 3865 (1996).
[24]M. J. Wenzel and G. Steinle-Neumann, Phys. Rev. B **75**, 214430 (2007).
[25]A. I. Liechtenstein, V. I. Anisimov, and J. Zaanen, Phys. Rev. B **52**, 5467 (1995).
[26]E. Nazarenko, J. E. Lorenzo, Y. Joly, J. L. Hodeau, D. Mannix, and C. Marin, Phys. Rev. Lett. **97**, 056403 (2006).
[27]J. P. Wright, J. P. Attfield, and P. G. Radaelli, Phys. Rev. B **66**, 214422 (2002).
[28]M. E. Fleet, Acta Crystallogr. Sec. B **37**, 917 (1981).
[29]Additional structural details. See Supplemental Material at http://link.aps.org/supplemental/10.1103/PhysRevB.87.155141 for details on atomic positions, a comparison of h-Fe_3O_4 space groups, other computational methods, the Hubbard U dependence, and computational relaxation choices. See also Refs. 38–41.
[30]P. Piekarz, K. Parlinski, and A. M. Oles, Phys. Rev. Lett. **97**, 156402 (2006).
[31]R. G. Burns, *Mineralogical Applications of Crystal Field Theory* (Cambridge University Press, Cambridge, 1993).
[32]A. van de Walle and G. Ceder, Rev. Mod. Phys. **74**, 11 (2002).
[33]J. Li, V. V. Struzhkin, H. K. Mao, J. F. Shu, R. J. Hemley, Y. W. Fei, B. Mysen, P. Dera, V. Prakapenka, and G. Y. Shen, Proc. Natl. Acad. Sci. USA **101**, 14027 (2004).
[34]A. Bengtson, K. Persson, and D. Morgan, Earth Planet. Sci. Lett. **265**, 535 (2008).
[35]K. Persson, A. Bengtson, G. Ceder, and D. Morgan, Geophys. Res. Lett. **33**, L16306 (2006).
[36]A. V. Krukau, O. A. Vydrov, A. F. Izmaylov, and G. E. Scuseria, J. Chem. Phys. **125**, 224106 (2006).
[37]M. Swart, J. Chem. Theory Comput. **4**, 2057 (2008).
[38]T. Kawakami, Y. Tsujimoto, H. Kageyama, X. Q. Chen, C. L. Fu, C. Tassel, A. Kitada, S. Suto, K. Hirama, Y. Sekiya, Y. Makino, T. Okada, T. Yagi, N. Hayashi, K. Yoshimura, S. Nasu, R. Podloucky, and M. Takano, Nat. Chem. **1**, 371 (2009).
[39]A. Bergner, M. Dolg, W. Kuchle, H. Stoll, and H. Preuss, Mol. Phys. **80**, 1431 (1993).
[40]Nathan Pinney, James D. Kubicki, Derek S. Middlemiss, Clare P. Grey, and Dane Morgan, Chem. Mater. **21**, 5727 (2009).
[41]T. Tsuchiya, R. M. Wentzcovitch, C. R. S. da Silva, S. de Gironeoli, and J. Tsuchiya, Phys. Status Solidi B **243**, 2111 (2006).